Knockout of the prion protein (PrP)-like *Sprn* gene does not produce embryonic lethality in combination with PrP^C-deficiency

Nathalie Daude[a], Serene Wohlgemuth[a], Rebecca Brown[b], Rose Pitstick[b], Hristina Gapeshina[a], Jing Yang[a], George A. Carlson[b], and David Westaway[a,c,d,1]

[a]Centre for Prions and Protein Folding Diseases, [c]Department of Biochemistry, and [d]Division of Neurology, Department of Medicine, University of Alberta, Edmonton, AB, Canada T6G 2M8; and [b]McLaughin Research Institute, Great Falls, MT 59405

Edited by Reed B. Wickner, National Institutes of Health, Bethesda, MD, and approved April 25, 2012 (received for review February 7, 2012)

The *Sprn* gene encodes Shadoo (Sho), a glycoprotein with biochemical properties similar to the unstructured region of cellular prion protein (PrP^C). Sho has been considered a candidate for the hypothetical π protein that supplies a PrP^C-like function to maintain the viability of $Prnp^{0/0}$ mice lacking the PrP^C protein. To understand these relationships more clearly we probed the cell biology of Sho and created knockout mice. Besides full-length and a "C1" C-terminal fragment, we describe a 6-kDa N-terminal Sho neuropeptide, "N1," which is present in membrane-enriched subcellular fractions of wild-type mice. *Sprn* null alleles were produced that delete all protein coding sequences yet spare the *Mtg*1 gene transcription unit that overlaps the *Sprn* 3′ UTR; the resulting mice bred to homozygosity were viable and fertile, although $Sprn^{0/0}$ mice maintained in two genetic backgrounds weighed less than wild-type mice. Lack of Sho protein did not affect prion incubation time. Contrasting with lethality reported for knockdown of expression in $Prnp^{0/0}$ embryos using lentiviruses targeted against the *Sprn* 3′ UTR, we established that double-knockout mice deficient in both Sho and PrP^C are fertile and viable up to 690 d of age. Our data reduce the impetus for equating Sho with the notional π protein and are not readily reconciled with hypotheses wherein expression of PrP^C and Sho are both required for completion of embryogenesis. Alternatively, and in accord with some reports for PrP^C, we infer that Sho's activity will prove germane to the maintenance of neuronal viability in postnatal life.

disease susceptibility | genetic redundancy | prion gene family

Prion infections result in a conformational remodeling of the cellular prion proteins (PrP^C) that yields a β-sheet–enriched and infectivity-associated form denoted PrP^{Sc} (1). In independent support of biochemical analyses, missense mutations in the PrP gene (*Prnp*) on chromosome 2 in mice impact disease progress and pathology (2–4). $Prnp^{0/0}$ mice have a normal development and are completely resistant to prion infections (5) and, although useful in the study of disease pathogenesis, have heightened curiosity as to PrP^C's function. Reported phenotypes in $Prnp^{0/0}$ mice are disparate and sometimes subtle: these include altered circadian rhythms (6, 7), sensitivity to oxidative stress (8), excitability of hippocampal neurons (9, 10), sensitivity to seizure (11, 12), age-related behavioral deficits (13–15), deficits in olfaction (16), and altered maintenance of the peripheral nervous system (17). The nonlethal effect of PrP^C-deficiency has provoked interest in the concept of functional degeneracy, with a hypothetical PrP functional homolog being deduced from genetic data and termed "π" (18, 19). More recently, the *Sprn* gene (20) on chromosome 7 has been shown to encode the Shadoo (Sho) glycoprotein with homology to the PrP^C hydrophobic domain. Sho, like PrP, is attached to the cell surface by a GPI anchor (21). In prion infections, levels of Sho protein are markedly reduced (21–24). In terms of physiological action, Sho, like PrP^C, can exhibit neuroprotective properties (21) and shares a number of binding partners in common with PrP^C (25). Importantly, in $Prnp^{0/0}$ embryos, *Sprn* knockdown using lentiviral vectors is reported to result in embryonic lethality (26). Spurred by these findings, we generated Shadoo-deficient mice. We report here that $Sprn^{0/0}$ animals with no detectable Sho protein display no overt malformation at birth or in adult life. Surprisingly, mice deficient in both Sho and PrP^C were also found to be viable as adults. Our data define constraints applying to the π hypothesis and the ways in which PrP^C and Sho might interact in the CNS.

Results and Discussion

Generation of $Sprn^{0/0}$ Mice. Generation of an *Sprn* null allele involved a deletion of noncoding exon 1 and the 5′ part of exon 2 containing all 444 bp of the *Sprn* protein coding sequence (the latter being replaced by a neomycin cassette), a strategy thus sparing the transcription unit of the overlapping *Mtg*1 gene (Fig. 1*A*, and Figs. S1 and S2). The targeting vector was transfected into 129Sv/Pas ES cells and two clones with correct targeting into chromosome 7 were microinjected into C57BL/6J blastocysts, resulting in chimeric mice that subsequently gave germ-line transmission to yield $Sprn^{0/wt}$ heterozygotes. Intercrosses of the heterozygotes in turn produced $Sprn^{0/0}$ mice that were born at the expected Mendelian distribution (Table S1); these homozygous null $Sprn^{0/0}$ mice showed no gross morphological alterations. Both male and female $Sprn^{0/0}$ mice were fertile (Table S1).

Prior analyses of *Sprn* gene expression have mainly focused upon mRNA transcripts, augmented by descriptions of full-length and C1 Sho protein fragments present in CNS samples (21). To extend these analyses, we surveyed for the presence and biochemical signature of Sho protein in peripheral tissues using $Sprn^{0/0}$ as negative controls; these studies used a diethylamine (DEA)-based fractionation used previously for amyloid precursor protein (APP) and secreted APP (sAPP) (27, 28) to yield membrane-associated (pellet) and membrane-dissociated (supernatant) fractions. The analyses failed to define expression of the Sho glycoprotein in organs other than the brain (Fig. S3), and thus fall in broad agreement with analyses of *Sprn* expression from reporter Tg mice (http://www.gensat.org). Accordingly, our subsequent experiments placed an emphasis upon neural structures. Western blot analysis of brain homogenates prepared from $Sprn^{0/0}$, $Sprn^{0/wt}$, and $Sprn^{wt/wt}$ mice established that no Sho protein was produced from the knockout allele, and that PrP^C levels were not affected by the lack of expression of Sho protein (Fig. 1*B*).

Author contributions: N.D., G.A.C., and D.W. designed research; N.D., S.W., R.B., R.P., H.G., and J.Y. performed research; N.D. and D.W. contributed new reagents/analytic tools; N.D. and D.W. analyzed data; and N.D., G.A.C., and D.W. wrote the paper.

The authors declare no conflict of interest.

This article is a PNAS Direct Submission.

Freely available online through the PNAS open access option.

[1]To whom correspondence should be addressed. E-mail: david.westaway@ualberta.ca.

This article contains supporting information online at www.pnas.org/lookup/suppl/doi:10.1073/pnas.1202130109/-/DCSupplemental.

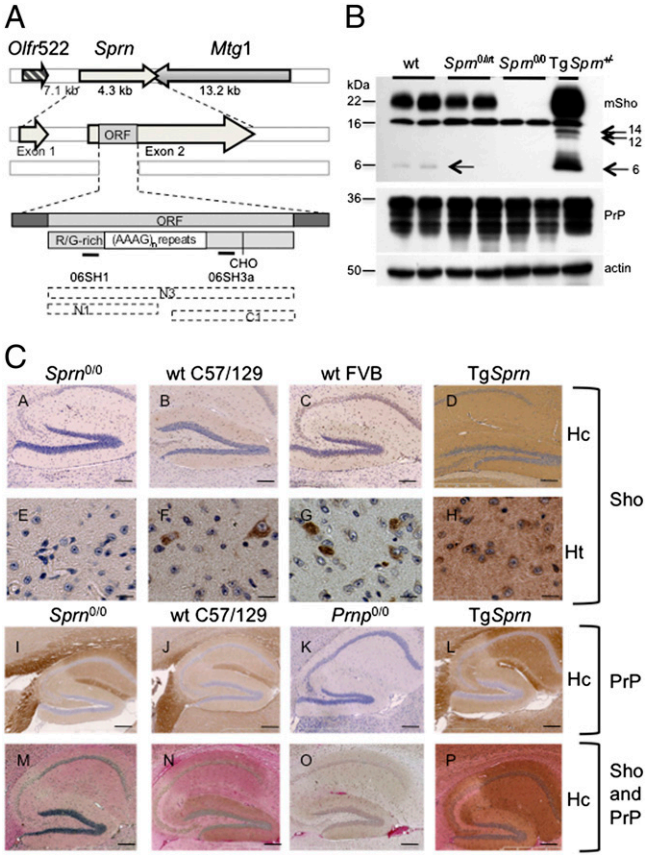

Fig. 1. Targeting construction and strategy. Generation of *Sprn*$^{0/0}$ mice. (*A*) Diagrammatic representation of genomic structure of *Sprn* locus and targeting vector. The targeting vector was constructed by replacing ~5.6 kb of genomic DNA downstream of the start codon, including exon 1 and the majority of exon 2, with a neomycin resistance gene flanked by loxP sequences. 06SH1 and 06Sh3a are the polyclonal antibodies, which have been raised against Sho. N3 corresponds to the full-length protein (mSho), N1 and C1 are processed fragments, N and C terminal, respectively. (*B*) Sho protein expression was assessed by immunoblotting of brain homogenates prepared from *Sprn*$^{0/0}$ *Sprn*$^{0/wt}$, *Sprn*$^{wt/wt}$ and Tg*Sprn*$^{+/-}$ mice. Arrows point to the 6-, 12-, and 14-kDa N1 fragment of Sho. Controls for protein loading are represented by analyses with anti-PrP and anti–β-actin antibodies. (*C*) Photomicrograph of sagittal section of hippocampus (Hc, A–D, I–P), hypothalamus (Ht, E–H), of wild-type C57/129, wild-type FVB, *Sprn*$^{0/0}$ and Tg*Sprn*$^{+/-}$ mice. Subpanels A to H demonstrate expression of Sho in normal brain (06SH1 antibody) and PrP^{C} expression in the hippocampus is depicted in subpanels J to L (Sha31 antibody). Double-labeling in subpanels M to P reveals the expression of both Sho (brown) and PrP (red). (Scale bars, 500 μm for Hc, 25 μm for Ht.)

Neuroanatomy of Sho Expression. Our next experiments focused on the neuroanatomy of Sho protein expression. Prior analyses used peptide competition of a polyclonal antibody as a control for specificity of immunostaining to wild-type tissue sections (21). Using a different N-terminal antibody preparation and using *Sprn*$^{0/0}$ mice as internal controls, we confirmed and extended aspects of the prior results. In the hippocampus of wild-type mice, Sho immunostaining was most readily apparent in the molecular layer of the dentate gyrus extending to the hippocampal fissure. PrP^{C}, on the other hand, was prominent in the molecular layer adjacent to CA1 neurons (Fig. 1*C*). These data elaborate on the concept that these two proteins do not always have coincident expression (21), and are of potential relevance to the issue of redundancy between *Sprn* and *Prnp* (see below). An additional finding during the course of these studies was a prominent staining of the cell body in some neurons of the lateral hypothalamus (Fig. 1*C*, subpanels F and G).

Prion Infection of *Sprn*$^{0/0}$ Mice. Prior studies have shown that overexpression of wild-type mouse Sho does not alter the outcome of infections with mouse-adapted prion isolates (21–23, 29). On the other hand, a *SPRN* frame-shift mutation—a putative null allele—was identified in two of 107 vCJD patients but not in 861 controls (30), suggesting a role for Sho in disease susceptibility in humans. The viability of *Sprn*$^{0/0}$ adult mice allowed us to test a possible role for endogenous Sho protein subsequent to challenge by mouse-adapted prions. *Sprn*$^{0/0}$, *Sprn*$^{0/wt}$, and *Sprn*$^{wt/wt}$ mice were inoculated with Rocky Mountain Laboratory (RML) prions by intracerebral (i.c.), intraperitoneal (i.p.), and oral routes (Fig. 2). Groups of i.c. inoculated mice had incubation times (± SEM) of 151 ± 6 d (wild-type, $n = 6$), 154 ± 5 d (*Sprn*$^{0/wt}$, $n = 10$), and 150 ± 5 d (*Sprn*$^{0/0}$, $n = 10$), and protease-resistant PrP species in brain homogenates were not notably different between the three genotypes (Fig. S4). Following i.p. inoculation, *Sprn* wild-type, ($n = 12$), *Sprn*$^{0/wt}$, ($n = 11$), and *Sprn*$^{0/0}$ ($n = 8$) mice had incubation times (± SEM) of 177 ± 2, 176 ± 5.5, and 179 ± 7 d, respectively. For the oral route, diagnosis by clinical signs was also similar for the three genotypes: *Sprn*$^{0/0}$ (203 ± 3 d, $n = 4$), *Sprn*$^{0/wt}$, (208 ± 7 d, $n = 9$), and wild-type (212 ± 11 d, $n = 6$) mice. This experiment was discontinued at 300 d before clinical signs developed in all of the gavaged mice of the cohort. Thus, in contrast to the causal relationships to disease pathogenesis that may exist for missense and frame-shift *SPRN* alleles in conjunction with human-tropic prions (30), absence of mouse Sho does not significantly impact the temporal and clinical manifestation of prion infections, at least for the RML prion isolate. This finding is in accord with studies using Tg.*Sprn* mice that overexpress Sho (22–24), and

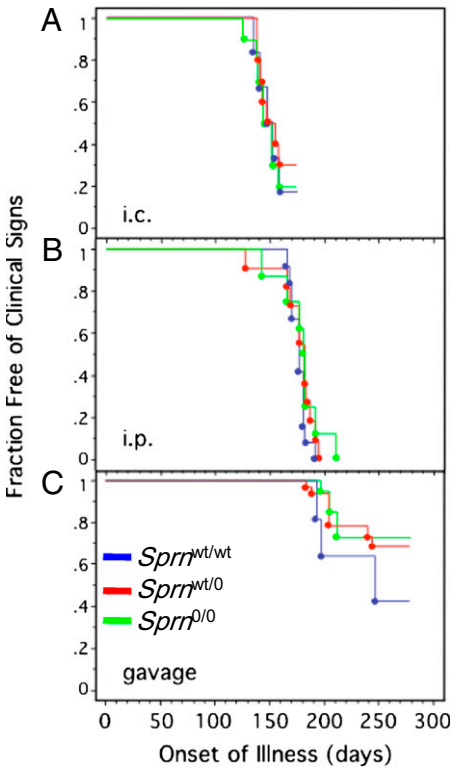

Fig. 2. Prion infection of *Sprn*$^{0/0}$ mice. Survival analysis following inoculation of wild-type, *Sprn*$^{0/wt}$, *Sprn*$^{0/0}$ mice with the RML isolate of mouse-adapted prions. (*A*) intracerebral route (ic), (*B*) intraperitoneal route (ip), (*C*) oral route (gavage).

underscores the conclusion that murine Sho does not play an active role in prion replication. Rather, we hypothesize that the notable "property" of endogenous mouse Sho in a prion infection is to reveal—by its own disappearance—the onset of a degradative activity directed against protease-resistant PrP^{Sc}.

Subcellular Fractionation of Sho Protein and a Membrane-Associated N-Terminal Fragment. A next series of experiments focused on molecular and neurobiological aspects of Sho protein expression. Brain tissue from wild-type and *Sprn*$^{0/0}$ mice were homogenized and fractionated by sequential centrifugation. We obtained similar results from frozen and freshly harvested tissue (not presented), with data from frozen tissue presented in Fig. 3*A*, and from mouse N2a neuroblastoma cells expressing wild-type Sho in Fig. 3*B*. Several features emerged from these analyses. First, full-length Sho (mSho) protein was dispersed across several fractions and was present within two fractions, F3 and F4, containing histones (i.e., indicative of the presence of nuclei). A second feature of the analyses was the presence of Sho protein fragments (i.e., absent in *Sprn*$^{0/0}$ samples) of 14, 12, and 6 kDa. The fragments of 14 and 12 kDa may correspond to protein species that have not been modified at the single *N*-linked glycosylation site, with the latter possibly representing a C-terminal truncation. The 6-kDa species (see also Fig. 1*B*) has not been reported previously and was investigated further. Sho is cleaved to a membrane-anchored C-terminal fragment denoted "C1" (following from the nomenclature for endoproteolytic fragments of PrP^{C}) (31), suggesting that the 6-kDa fragment detected by 06rSH1 antibody might comprise the reciprocal "N1" proteolytic product. In prior analyses and experiments presented in Fig. 3*C*, DEA extraction was used to separate membrane-tethered and extrinsic/secreted forms of APP (27, 28) and Sho (22), but low M_r Sho species were not scrutinized. Here, examination of DEA extracts from whole brain and from dissected olfactory bulb, pituitary, and cerebellum homogenates revealed a 6-kDa fragment of Sho in the pellet fraction of Tg*Sprn* mice (and in wild-type mice, but not in *Sprn*$^{0/0}$ mice, after longer autoradiographic exposures). The presence of an N1 fragment in a membrane-associated pellet fraction was unexpected because the size precludes the presence of a GPI anchor. We speculate that the N1 fragment might be present inside vesicles or, if the hydrophobic region is present within the N1 fragment, that this region can form a transmembrane helix.

Body Mass in *Sprn*$^{0/0}$ Mice. Growth curves for body weight in *Sprn*$^{0/0}$ mice differed from controls (Tables 1 and 2). Young mice show a biphasic growth curve with an inflection point at the time of weaning. Across all data there was a significant interaction between genotype and body weight ($P < 0.05$). For females significance was in the first phase of growth, with the situation reversed for males. With initial data obtained from an outbred 129Pas/C57BL6 background, we extended the study to cohorts where the *Sprn* null allele had mobilized by seven backcrosses and four generations of inbreeding (N7, F4) to an FVB/NCr genetic background. Here, an effect upon body weight was apparent in young adult homozygous null animals, wherein a decrement of about 9% was noted versus control wild-type littermate animals, reaching significance in males ($P < 0.05$). These data argue for a relationship between levels of Sho expression (arising here from different *Sprn* gene dosage) and body mass. Interestingly, another biological context where expression of Sho protein is reduced in the instance of prion infections (21–24). Although Sho down-regulation could be dissociated temporally from neurological signs used to diagnose end-stage disease (22, 23), we note that prion disease can also be associated with changes outside of the CNS: specifically, a number of prion strains produce a loss in body mass, and less commonly, some strains produce an increase (32, 33). Further studies will be needed to ascertain whether Sho levels are altered in hypothalamic neurons of mice infected with different prion strains and, if alterations are evident, whether or not there is a consistent relationship with perturbed body mass.

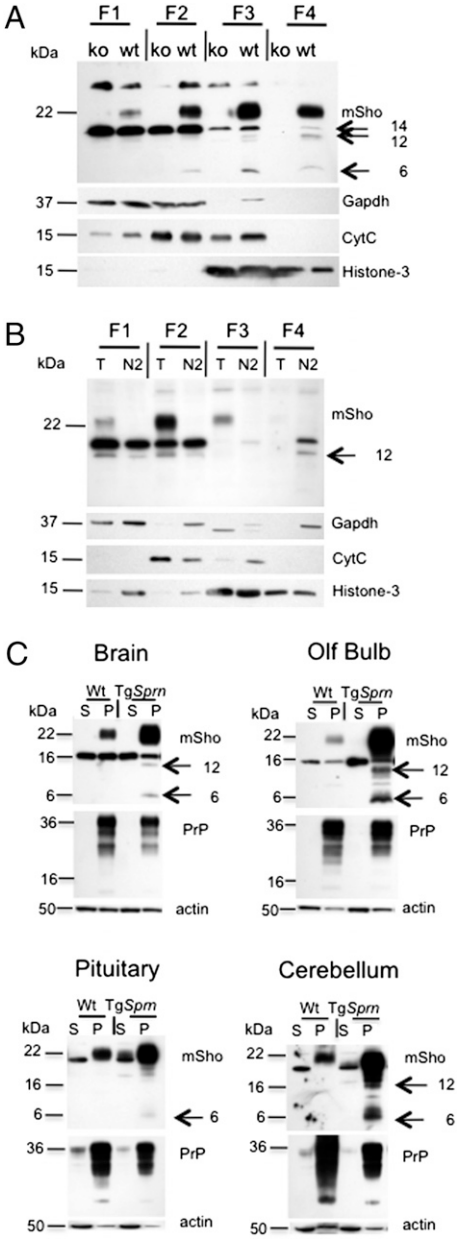

Fig. 3. Behavior of Sho protein in subcellular fractionations. Immunoblots showing subcellular distribution of Sho in (*A*) brain of *Sprn*$^{0/0}$ and wild-type mice, and (*B*) in N2a neurobastoma cells that are either wild-type (N2), or overexpressing a mouse Sho transgene (T). An arrow points to the 6-, 12-, and 14-kDa N1 Sho fragment and mature glycosylated Sho is denoted "mSho." The subcellular fractions correspond to cytoplasm (F1), membrane (F2), nucleus (F3), and cytoskeleton (F4). Equivalent Western blots indicating the relative distribution of various subcellular localization markers: cytochrome C (mitochondrial, membrane), Gapdh (cytosolic), and Histone H3 (nuclear). (*C*) Immunoblot representing DEA fractionation of tissue homogenates from wt and Tg*Sprn*$^{+/-}$ mice. S and P represent supernatant and pellet, respectively. Tissues correspond to brain, olfactory bulb, pituitary, and cerebellum. An arrow points to processed Sho *N*-ter fragment of 6-, 12-, and 14-kDa. Membranes were reprobed for expression of PrP and β-actin.

Generation of *Sprn*$^{0/0}$ Plus *Prnp*$^{0/0}$ Double-Knockout Mice. Because an earlier report described a lethal phenotype resulting from knockdown of Sho mRNA expression in *Prnp*$^{0/0}$ embryos (26), we crossed *Sprn*$^{0/0}$ mice with FVB.129-*Prnp*^{tm1Zrch} (*Prnp*$^{0/0}$) mice to verify the hypothesis that *Sprn*$^{0/0}$ *Prnp*$^{0/0}$ mice are embryonic lethal. Surprisingly, double-knockout mice were viable, fertile, and produced in crosses at the expected Mendelian ratios (Table S1). Sequential crosses performed over multiple generations excluded the possibility that viability was a transient phenomenon, for example one perpetuated by carry-over of maternal mRNAs encoded by *Sprn*$^{0/wt}$ heterozygotes. Protein analyses of *Sprn*$^{0/0}$ plus *Prnp*$^{0/0}$ mice are shown in Fig. 4*A*. Although *Prnp* and *Sprn* may encode proteins with overlapping activities (as discussed below), their activities are not interrelated to the extent that their expression levels are counterbalanced. The concept that lack of PrP^C produces an increase in Sho expression has been excluded previously by protein analyses of the CNS in *Prnp*$^{0/0}$ mice (21, 22, 29), and here we can exclude that an alteration in *Sprn* gene dosage (and hence Sho protein level) affects CNS levels of PrP^C (Fig. 4). Gross brain morphology was similar to wild-type in *Sprn*$^{0/0}$, *Prnp*$^{0/0}$, and *Sprn*$^{0/0}$ *Prnp*$^{0/0}$ mice (Fig. S5). Groups of *Sprn*$^{0/0}$ *Prnp*$^{0/0}$ (n = 10), *Sprn*$^{0/0}$ *Prnp*$^{0/wt}$ (n = 11), and *Sprn*$^{0/wt}$ *Prnp*$^{0/0}$ (n = 10) mice were aged and observed for behavioral abnormalities. All mice appeared normal until 295 d. Subsequent to this age, *Prnp*$^{0/wt}$ mice homozygous for the *Sprn* null allele did not show neurological signs, whereas *Prnp*$^{0/0}$ mice exhibited neurological signs that included tremors, paw clasping when lifted by the tail, dysmetria, or mild ataxia, regardless of whether they were homozygous or heterozygous for the *Sprn* null allele. In agreement with prior descriptions (17, 34), necropsy revealed dysmyelination and a granulomatous infiltrate in the lateral horns of the spinal cord in two affected *Prnp*$^{0/0}$ mice at 672 d (*Sprn*$^{0/0}$) and 694 d (*Sprn*$^{0/wt}$), but none in a *Prnp*$^{0/wt}$ *Sprn*$^{0/0}$ mouse at 694 d. We have not observed these signs in our inbred FVB.*Prnp*$^{0/0}$ colonies, although we rarely maintain mice this long. Cross-sections of sciatic nerve revealed morphology akin to wild-type controls in *Sprn*$^{0/0}$ mice, versus similar degrees of dysmyelination and irregular fiber diameters in aged *Prnp*$^{0/0}$ mice and *Sprn*$^{0/0}$ *Prnp*$^{0/0}$ mice (Fig. 4*B*), indicating that absence of Sho does not accentuate a phenotype associated with lack of PrP^C in adult mice.

Activities Needed to Maintain Cell Viability in the Adult CNS and in Mouse Embryos. To account for toxic properties of internally-deleted PrP^C causing cerebellar degeneration and the lack of an overt phenotype in *Prnp*$^{0/0}$ mice, a model has been proposed wherein PrP^C docks to a hypothetical membrane protein L_{PrP} to initiate intracellular signals that maintain cell viability, with a second hypothetical molecule π supplying a PrP-like function when PrP^C is removed by genetic deletion (18). In terms of known PrP-like molecules, Doppel is barely expressed in the CNS in wild-type mice (35, 36) and can be excluded from consideration. However, because Sho is expressed in the CNS (21 and present study) and has a number of PrP^C-like biochemical properties (21, 25, 37), it is considered as a candidate for π. Indeed, the report of embryonic lethality from knockdown of Sho in *Prnp*$^{0/0}$ embryos (26) added impetus to this notion. On the other hand, our data demonstrate that mice fully deficient in both Sho and PrP^C are viable. To appraise these issues we will consider technical aspects of gene ablation before turning to the current state of the L_{PrP}/π hypothesis.

In a seeming paradox, the genetically "leaky" procedure of combining a *Prnp*$^{0/0}$ genotype with a transient lentiviral knockdown of *Sprn*, verified by analysis of RNA levels, is reported (26) as generating a stronger phenotype (i.e., embryonic lethality) than a procedure of breeding to homozygosity for constitutive null alleles of both *Sprn* and *Prnp* (here, with all of the *Sprn* coding region deleted) and with lack of *Sprn* expression verified by analysis of Sho protein (Fig. 4). How might this puzzling divergence in outcomes arise? Both studies use the *Zrch*1 null

Table 1. Analysis of body weight in Sho-deficient mice: C57BL/129 genetic background

Sex	Type	Age (d) 8	10	12	14	16	18	20	22	24	26	28	30	32	34	36	38	40	42
Female	wt C57	6.61 ± 0.38	8.14 ± 0.38	9.44 ± 0.39	10.36 ± 0.30	10.36 ± 0.36	10.86 ± 0.31	11.75 ± 0.33	12.80 ± 0.29	14.16 ± 0.32	15.50 ± 0.35	16.58 ± 0.36	17.69 ± 0.34	18.89 ± 0.34	19.63 ± 0.30	20.28 ± 0.35	20.72 ± 0.24	21.20 ± 0.30	21.18 ± 0.34
	Sprn0/+	5.73 ± 0.25	7.10 ± 0.25	8.38 ± 0.24	9.31 ± 0.25	9.45 ± 0.25	9.83 ± 0.30	10.63 ± 0.34	11.74 ± 0.36	13.16 ± 0.40	14.61 ± 0.44	15.93 ± 0.45	17.00 ± 0.44	18.19 ± 0.44	19.12 ± 0.43	19.73 ± 0.39	20.30 ± 0.37	20.71 ± 0.36	20.96 ± 0.37
	Sprn0/0	5.62 ± 0.12*	6.87 ± 0.18*	7.99 ± 0.24*	8.76 ± 0.29*	9.35 ± 0.31*	9.91 ± 0.32	10.86 ± 0.31	11.99 ± 0.32	13.41 ± 0.34	14.82 ± 0.34	15.97 ± 0.34	17.09 ± 0.34	18.21 ± 0.34	18.98 ± 0.34	19.58 ± 0.34	20.12 ± 0.31	20.44 ± 0.31	20.91 ± 0.32
Male	wt C57	6.08 ± 0.38	7.58 ± 0.38	9.08 ± 0.39	10.14 ± 0.30	10.46 ± 0.36	10.91 ± 0.31	11.84 ± 0.25	13.27 ± 0.18	15.54 ± 0.26	18.08 ± 0.26	20.57 ± 0.31	22.61 ± 0.44	24.35 ± 063	25.47 ± 0.78	26.27 ± 0.87	26.88 ± 1.01	27.58 ± 0.99	28.14 ± 1.07
	Sprn0/+	5.86 ± 0.26	7.33 ± 0.297	8.66 ± 0.31	9.71 ± 0.34	9.88 ± 0.29	10.32 ± 0.29	11.27 ± 0.32	12.5 ± 0.38	14.38 ± 0.43	16.67 ± 0.51	18.83 ± 0.58	20.70 ± 0.58	22.27 ± 0.56	23.28 ± 0.542	23.98 ± 0.56	24.57 ± 0.59	25.06 ± 0.60	25.45 ± 0.64
	Sprn0/0	5.66 ± 0.15	6.91 ± 0.17	8.02 ± 0.23	8.89 ± 0.23	9.53 ± 0.23	10.07 ± 0.21	11.00 ± 0.22	12.37 ± 0.23	14.33 ± 0.24	16.59 ± 0.29	18.82 ± 0.29*	20.78 ± 0.27*	22.31 ± 0.26*	23.30 ± 0.25*	23.89 ± 0.23*	24.43 ± 0.24*	24.97 ± 0.28*	25.41 ± 0.30*

*P value <0.05.

Table 2. Analysis of body weight in Sho-deficient mice: FVB/NCr genetic background

Sex	Type	Age (d) 15	22	29	36	43	50
Female	wt FVB	7 ± 0.31	12 ± 0.84	17.22 ± 0.36	20.22 ± 0.40	20.77 ± 0.46	22 ± 0.24
	Sprn*0/0*	9.25 ± 0.47	11.6 ± 0.47	17.3 ± 0.33	19.5 ± 0.37	20.85 ± 0.46	22.28 ± 0.68
Male	wt FVB	7.8 ± 0.33	14.38 ± 0.36	20.84 ± 0.46	24.07 ± 0.43	25.84 ± 0.54	27.23 ± 0.58
	Sprn*0/0*	7.66 ± 0.20	11.64 ± 0.69**	19.28 ± 0.42*	22.07 ± 0.29**	23.75 ± 0.27**	25 ± 0.28**

*P value <0.05; **P value <0.01.

allele of *Prnp*, thus excluding a phenomenon wherein some *Prnp* null alleles affect RNA splicing to the adjacent *Prnd* locus thus encoding the neurotoxic Doppel protein (36). Genetic background is similar, but not identical, being FVB/N for the knockdown studies versus FVB/NCr × 129Pas used in the studies here. "Off-axis" effects from an individual *Sprn*-targeting lentiviral vector (38, 39) could be considered but the use of two independent shRNA lentiviruses to obtain a similar phenotypic outcome (26) tempers this interpretation. In the theoretical realm, it is possible that transient knockdown of *Sprn* expression could produce a stronger phenotype than a constitutive null allele if the absence of Sho early in embryogenesis (as would be the case for a constitutive null allele) were to induce expression of protein with a similar functionality, such that a later developmental checkpoint between e8 and e11 could be overcome, even though Sho is knocked down. A last possibility considers genetic strategies: targeting the *Sprn* 3′ UTR by knockdown, versus deletion of protein coding sequence. Since the *Sprn* gene overlaps the transcriptionally opposed *Mtg1* gene, interventions targeting the *Sprn* 3′UTR could well perturb the abundance of *Mtg1* transcripts. Consequent alterations in expression of the Mtg1 protein might then prove deleterious to embryo development in concert with removal of a protective action attributed to PrP^C.

Because caveats pertaining to *Mtg*1 do not apply to our gene targeting strategy, we can return to a consideration of the π hypothesis. As we now demonstrate that $Prnp^{0/0}$ $Sprn^{0/0}$ double-knockout mice have normal brain neuroanatomy (Fig. S5), and that Sho and PrP^C expression are not always coincident (Fig. 1*C*), then within the framework of the hypothesis it follows that Sho is not π. Perhaps other proteins should now be auditioned for this role (e.g., ref. 40). However, it is also to be considered whether the original formulation of the π hypothesis is compatible with our current knowledge of PrP^C chemistry. For example, the π hypothesis envisages two discrete, covalently linked binding sites on PrP^C (one N terminal, one C terminal) simultaneously docking onto the L_{PrP} protein, yet we now know that much of PrP^C at steady-state is endoproteolysed to separate the N- and C-terminal domains (31, 41–43). Furthermore, other hypotheses that also seek to explain the properties of internal PrP deletions neither invoke a PrP paralog nor consider action in embryonic development (44). Rather, although there is data that the zebrafish PrP-1 gene may modulate cell adhesion and serve a neurodevelopmental role (45), there is a broad consensus that PrP^C in mammals may serve to protect or maintain neurons in adult life (46). The same concept may apply to Sho as well, and experiments to appraise this possibility are underway.

Materials and Methods

Animal Husbandry and Prion Inoculations. The animals were housed in groups up to five under a 12-h light/dark cycle with food and water ad libitum. All animal protocols were in accordance with the Canadian Council on Animal Care or the Guide for the Care and Use of Laboratory Animals (National Institutes of Health, US Public Health Service) and were approved by the Institutional Animal Care and Use Committees at the University of Alberta and McLaughlin Research Institute (MRI). MRI is fully accredited by the International American Association for the Accreditation of Laboratory Animal Care International. Prion inoculations [30 μL of 1% (wt/vol) brain homogenate for intracerebral, 300 μL for intraperitoneal and oral infections] and clinical diagnoses were done as described previously (47). Results are reported as mean ± SEM. $P < 0.05$ was considered as significant. One-way ANOVA followed by post hoc t tests with corrections for multiple comparisons was used for body weight measurements.

Generation of Targeted Vector. Our gene-targeting strategy was designed by GenOway and is described in *SI Materials and Methods*. All vectors used are shown in Fig. S1.

Western Blot Analyses. Whole brains of adult mice were homogenized in 0.32 M sucrose with protease inhibitors (Complete tablet; Roche Diagnostics). Whole extracts (50 μg of total protein) were subject to 14% SDS/PAGE and transferred to a PVDF membrane (Millipore). Immunodetection using the enhanced chemiluminescence (ECL) method (Pierce) was performed according to the manufacturer's instruction. The membrane was probed first with anti-Sho antibody (06r-SH1 or 06rSH3a) (21) and then anti-PrP (SHA31, Spi-

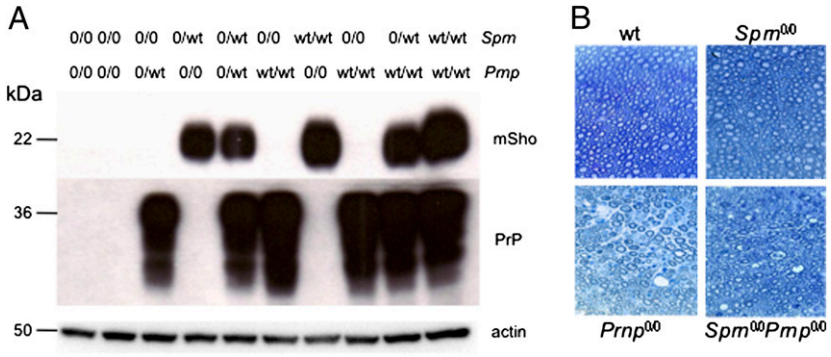

Fig. 4. Properties of double-knockout $Sprn^{0/0}$, $Prnp^{0/0}$ mice. (*A*) Western blot assays of endogenous Sho (06SH1) and PrP^C (Sha31) of adult mouse brain homogenates derived from different combinations of *Sprn* and *Prnp* genotypes. A β-actin blot demonstrates normalized protein loading. (*B*) Toluidine blue staining of semithin sections of sciatic nerve tissue from aged wild-type, $Sprn^{0/0}$, $Prnp^{0/0}$, and double-knockout $Sprn^{0/0}$ plus $Prnp^{0/0}$ mice. (Scale bar, 50 μm.)

bio), anti–β-actin (Sigma). Secondary antibodies used were horseradish peroxidase-conjugated anti-rabbit and anti-mouse (Bio-Rad).

Subcellular Fractionation. Brains from *Sprn*$^{0/0}$ mice, wild-type control C57/129 mice, as well as N2a cells stably expressing mouse Sho and wild-type N2a cells were homogenized and fractionated using the ProteoExtract Subcellular Proteome Extraction Kit (Calbiochem) into cytoskeletal, cytosol, membrane, and nuclear proteins. Subcellular fractions were equalized and immunoblotted subsequently with anti-Sho (06-SH1), anti-Cytochrome C (BD Pharmigen), anti-Gapdh (Sigma), anti-Histone H3 (Santa Cruz Biotechnology) antibodies.

Histology. Each specimen was fixed by immersion either in neutrally buffered 10% formalin or in Carnoy's fixative. Samples were subsequently dehydrated and routinely processed in paraffin. For morphological studies, conventional histological staining methods of H&E were used. Sections were treated with antibodies against Sho (06SH-1), PrP (SHA31), followed by detection using EnVision+ System-HRP (DAB) and ARK kits (Dako). For double labeling, Sho (06SH1) immunoreactivity was labeled with DAB, and PrP (SAF83) with alkaline phosphatase mediated activation of Vector Red stain (Vectorlabs).

DEA Extraction. DEA extraction of Sho from mouse brains was performed by a method previously described (27, 28). Briefly, brains were homogenized 10% wt/vol in 0.2% DEA in 50 mM NaCl. Homogenate was ultracentrifuged at 100,000 × *g* for 1 h at 4 °C. The resulting supernatant was neutralized with the addition of 0.5 M Tris-HCl pH 6.8 at a volume one-tenth that of the total. Pellets were resuspended in buffer of 50 mM Tris (pH 7.5), 0.5% sodium deoxycholate, and 0.5% Triton X-100 with proteases inhibitors.

ACKNOWLEDGMENTS. We thank Tom Duggan for technical assistance. This work was supported by funds from the Canadian Institutes for Health Research (MOP36377), PrioNet Networks of Centres of Excellence, the Alberta Heritage Foundation for Medical Research, and the Alberta Prion Research Institute (D.W.); and National Institutes of Health Grant NS41997 (to G.A.C.).

1. Cohen FE, Prusiner SB (1998) Pathologic conformations of prion proteins. *Annu Rev Biochem* 67:793–819.
2. Carlson GA, et al. (1986) Linkage of prion protein and scrapie incubation time genes. *Cell* 46:503–511.
3. Hunter N, Hope J, McConnell I, Dickinson AG (1987) Linkage of the scrapie-associated fibril protein (PrP) gene and Sinc using congenic mice and restriction fragment length polymorphism analysis. *J Gen Virol* 68:2711–2716.
4. Westaway D, et al. (1987) Distinct prion proteins in short and long scrapie incubation period mice. *Cell* 51:651–662.
5. Büeler H, et al. (1993) Mice devoid of PrP are resistant to scrapie. *Cell* 73:1339–1347.
6. Tobler I, et al. (1996) Altered circadian activity rhythms and sleep in mice devoid of prion protein. *Nature* 380:639–642.
7. Tobler I, Deboer T, Fischer M (1997) Sleep and sleep regulation in normal and prion protein-deficient mice. *J Neurosci* 17:1869–1879.
8. Klamt F, et al. (2001) Imbalance of antioxidant defense in mice lacking cellular prion protein. *Free Radic Biol Med* 30:1137–1144.
9. Colling SB, Collinge J, Jefferys JG (1996) Hippocampal slices from prion protein null mice: disrupted Ca(2+)-activated K+ currents. *Neurosci Lett* 209:49–52.
10. Mallucci GR, et al. (2002) Post-natal knockout of prion protein alters hippocampal CA1 properties, but does not result in neurodegeneration. *EMBO J* 21:202–210.
11. Walz R, et al. (1999) Increased sensitivity to seizures in mice lacking cellular prion protein. *Epilepsia* 40:1679–1682.
12. Rangel A, et al. (2007) Enhanced susceptibility of Prnp-deficient mice to kainate-induced seizures, neuronal apoptosis, and death: Role of AMPA/kainate receptors. *J Neurosci Res* 85:2741–2755.
13. Coitinho AS, Roesler R, Martins VR, Brentani RR, Izquierdo I (2003) Cellular prion protein ablation impairs behavior as a function of age. *Neuroreport* 14:1375–1379.
14. Lobão-Soares B, et al. (2008) Cellular prion protein modulates defensive attention and innate fear-induced behaviour evoked in transgenic mice submitted to an agonistic encounter with the tropical coral snake *Oxyrhopus guibei*. *Behav Brain Res* 194: 129–137.
15. Criado JR, et al. (2005) Mice devoid of prion protein have cognitive deficits that are rescued by reconstitution of PrP in neurons. *Neurobiol Dis* 19:255–265.
16. Le Pichon CE, et al. (2009) Olfactory behavior and physiology are disrupted in prion protein knockout mice. *Nat Neurosci* 12:60–69.
17. Bremer J, et al. (2010) Axonal prion protein is required for peripheral myelin maintenance. *Nat Neurosci* 13:310–318.
18. Shmerling D, et al. (1998) Expression of amino-terminally truncated PrP in the mouse leading to ataxia and specific cerebellar lesions. *Cell* 93:203–214.
19. Flechsig E, Weissmann C (2004) The role of PrP in health and disease. *Curr Mol Med* 4:337–353.
20. Premzl M, et al. (2003) Shadoo, a new protein highly conserved from fish to mammals and with similarity to prion protein. *Gene* 314:89–102.
21. Watts JC, et al. (2007) The CNS glycoprotein Shadoo has PrP(C)-like protective properties and displays reduced levels in prion infections. *EMBO J* 26:4038–4050.
22. Westaway D, et al. (2011) Down-regulation of Shadoo in prion infections traces a pre-clinical event inversely related to PrP(Sc) accumulation. *PLoS Pathog* 7:e1002391.
23. Watts JC, et al. (2011) Protease-resistant prions selectively decrease Shadoo protein. *PLoS Pathog* 7:e1002382.
24. Miyazawa K, Manuelidis L (2010) Agent-specific Shadoo responses in transmissible encephalopathies. *J Neuroimmune Pharmacol* 5:155–163.
25. Watts JC, et al. (2009) Interactome analyses identify ties of PrP and its mammalian paralogs to oligomannosidic N-glycans and endoplasmic reticulum-derived chaperones. *PLoS Pathog* 5:e1000608.
26. Young R, et al. (2009) The prion or the related Shadoo protein is required for early mouse embryogenesis. *FEBS Lett* 583:3296–3300.
27. Eckman EA, Watson M, Marlow L, Sambamurti K, Eckman CB (2003) Alzheimer's disease beta-amyloid peptide is increased in mice deficient in endothelin-converting enzyme. *J Biol Chem* 278:2081–2084.
28. Savage MJ, et al. (1998) Turnover of amyloid beta-protein in mouse brain and acute reduction of its level by phorbol ester. *J Neurosci* 18:1743–1752.
29. Wang H, et al. (2011) Overexpression of Shadoo protein in transgenic mice does not impact the pathogenesis of scrapie. *Neurosci Lett* 496:1–4.
30. Beck JA, et al. (2008) Association of a null allele of SPRN with variant Creutzfeldt-Jakob disease. *J Med Genet* 45:813–817.
31. Chen SG, et al. (1995) Truncated forms of the human prion protein in normal brain and in prion diseases. *J Biol Chem* 270:19173–19180.
32. Outram GW (1972) Changes in drinking and feeding habits of mice with experimental scrapie. *J Comp Pathol* 82:415–427.
33. Kim YS, Carp RI, Callahan SM, Wisniewski HM (1987) Scrapie-induced obesity in mice. *J Infect Dis* 156:402–405.
34. Nishida N, et al. (1999) A mouse prion protein transgene rescues mice deficient for the prion protein gene from purkinje cell degeneration and demyelination. *Lab Invest* 79:689–697.
35. Silverman GL, et al. (2000) Doppel is an N-glycosylated, glycosylphosphatidylinositol-anchored protein. Expression in testis and ectopic production in the brains of *Prnp*(0/0) mice predisposed to Purkinje cell loss. *J Biol Chem* 275:26834–26841.
36. Moore RC, et al. (1999) Ataxia in prion protein (PrP)-deficient mice is associated with upregulation of the novel PrP-like protein doppel. *J Mol Biol* 292:797–817.
37. Daude N, et al. (2010) Wild-type Shadoo proteins convert to amyloid-like forms under native conditions. *J Neurochem* 113:92–104.
38. Jackson AL, et al. (2003) Expression profiling reveals off-target gene regulation by RNAi. *Nat Biotechnol* 21:635–637.
39. Scacheri PC, et al. (2004) Short interfering RNAs can induce unexpected and divergent changes in the levels of untargeted proteins in mammalian cells. *Proc Natl Acad Sci USA* 101:1892–1897.
40. Schmitt-Ulms G, Ehsani S, Watts JC, Westaway D, Wille H (2009) Evolutionary descent of prion genes from the ZIP family of metal ion transporters. *PLoS ONE* 4:e7208.
41. Guillot-Sestier MV, Sunyach C, Druon C, Scarzello S, Checler F (2009) The alpha-secretase-derived N-terminal product of cellular prion, N1, displays neuroprotective function in vitro and in vivo. *J Biol Chem* 284:35973–35986.
42. Sunyach C, Cisse MA, da Costa CA, Vincent B, Checler F (2007) The C-terminal products of cellular prion protein processing, C1 and C2, exert distinct influence on p53-dependent staurosporine-induced caspase-3 activation. *J Biol Chem* 282:1956–1963.
43. Oliveira-Martins JB, et al. (2010) Unexpected tolerance of alpha-cleavage of the prion protein to sequence variations. *PLoS ONE* 5:e9107.
44. Li A, et al. (2007) Neonatal lethality in transgenic mice expressing prion protein with a deletion of residues 105-125. *EMBO J* 26:548–558.
45. Málaga-Trillo E, et al. (2009) Regulation of embryonic cell adhesion by the prion protein. *PLoS Biol* 7:e55.
46. Lo RY, et al. (2007) New molecular insights into cellular survival and stress responses: Neuroprotective role of cellular prion protein (PrPC). *Mol Neurobiol* 35:236–244.
47. Carlson GA, et al. (1994) Prion isolate specified allotypic interactions between the cellular and scrapie prion proteins in congenic and transgenic mice. *Proc Natl Acad Sci USA* 91:5690–5694.